

PHOTOMETRIC SIGNATURES OF LIQUID WATER IN JSC MARS-1 REGOLITH SIMULANT. K. Gunderson¹, B. Lüthi¹, P. Russell¹ and N. Thomas¹. ¹Physikalisches Institut, University of Bern, Sidlerstrasse 5, CH-3012 Bern, Switzerland (kurt.gunderson@luethi@patrick.russell@nicolas.thomas@space.unibe.ch).

Introduction: Subsurface polar ice deposits are believed to exist on Mars. Their existence has been predicted [1] and also has been inferred from remote sensing instruments [2–4]. Because of the low mean surface temperatures and low mean atmospheric pressures, liquid water might not be expected to exist on Mars. However, models suggest that solar heating can raise temperature and pressure conditions across much of the Martian surface such that the triple point of water can be exceeded without reaching the boiling point, especially if the water contains dissolved salts [5]. Laboratory simulations support this prediction [6]. Near the poles the solar heating conditions that could lead ice to melt are less likely to occur than in equatorial regions but, under consideration of evidence for recent volcanic activity on Mars [7–8], it is conceivable that geothermal sources could melt ice in localized polar regions and lead to short lived surface seepage.

As demonstrated in Figure 1, liquid water has a tendency to darken soils that absorb it. We attempt to quantify this darkening effect by comparing the bidirectional reflectance distribution functions (BRDFs) of dry and wet JSC Mars-1 regolith simulant [9] in a variety of optical bandpasses. The associated reflectance signatures of moisture in a regolith simulant could help identify regions of surface moisture, if they exist, in visible or near infrared (NIR) images of Mars.



Figure 1. Wet (left) and dry (right) JSC Mars-1 simulant.

Data and analysis: Measurements were made using the Physikalisches Institut Radiometric Experiment (PHIRE) [10]. PHIRE is a goniometer experiment that can illuminate and observe a test sample over a broad range of measurement geometries. The measurements described here were performed at an incidence angle of $i=50$ deg and over a range of in-plane phase angles from $2 \leq g \leq 130$ deg. Eight broadband optical filters, covering blue to NIR wavelengths, provided wavelength control over the illuminating beam. The filter set included both astronomical standards and analogs to the filter set being used by the HiRISE experiment

[11] aboard the Mars Reconnaissance Orbiter, and is summarized in Table 1. Hapke reflectance models [12] were fit to the data using six free parameters. Reduced BRDF data are shown in Figures 2 and 3 with model fits overplotted. Discrepancies between the models and data are typically less than a part in 100. The most striking difference between the BRDFs of the dry and

Table 1. Summary of the optical filter set.

Effective wavelength	Description
462 nm	Johnson <i>B</i> .
503 nm	HiRISE blue-green analog (<i>B_{HR}</i>).
558 nm	Johnson <i>V</i> .
672 nm	Johnson <i>R</i> .
736 nm	HiRISE red analog (<i>R_{HR}</i>).
777 nm	Kron-Cousins red (<i>R_{KC}</i>).
875 nm	Johnson <i>I</i> .
926 nm	HiRISE NIR analog (<i>I_{HR}</i>).

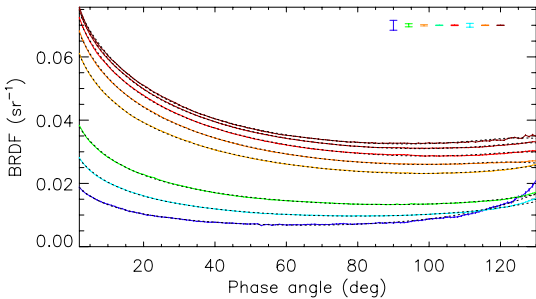


Figure 2. Measured BRDFs of dry JSC Mars-1 regolith simulant (colored lines) with reflectance models overplotted (dotted). Colors and effective wavelength values (nm) are: Blue=462, light blue=503, green=558, yellow-orange=672, orange=736, red=777, brown=875, dark brown=926. Systematic error bars are in the upper right corner.

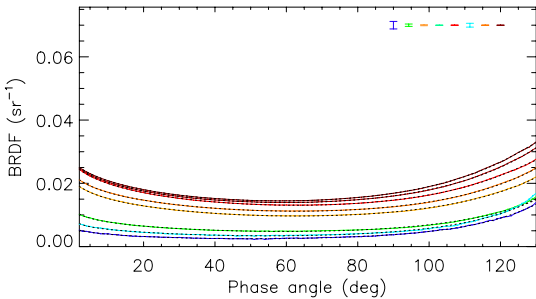


Figure 3. Same as Figure 2, but for wet JSC Mars-1 simulant.

wet samples is the relative weakness of the opposition surge in the wet sample. This is unusual for planetary regoliths and laboratory simulants.

Discussion: Figures 4 and 5 show a comparison of the JSC Mars-1 albedo measurements of [9] with albedo extrapolations of our best-fitting reflectance models to zero phase angles. The agreement between the measurements of [9] and our measurements of the dry simulant supports the validity of the PHIRE data. Discrepancies are most likely attributable to systematic uncertainties in the illumination source's output spectrum and photodiode QE, both of which were taken from vendor documentation to determine the effective wavelength values in Table 1. Also shown is a comparison between the regolith simulant measurements and measurements of dark and bright regions of the actual Martian surface [13]. The simulant is consistently darker than both the dry sample and a typical dark Martian surface region in all optical bandpasses.

Figure 6 shows the ratio of the BRDF of dry simulant to wet simulant. These data suggest that, if viewed from an orbiting platform, the brightness contrast between a localized region of wet regolith surrounded by mineralogically similar dry regolith would be stronger at low phase angles. At high phase angles, however, the wet and dry regions would be nearly equally bright. Contrast also appears higher at shorter wavelengths, but the significance of this wavelength trend is less certain because of systematic uncertainties in the data reduction methodology.

Conclusions: Photometric measurements of dry and wet Martian regolith simulant have been used to explore how localized regions of surface moisture on Mars might appear in visible/NIR images. The data, as expected, show that a wet region in a mineralogically uniform regolith would appear darker than the surrounding dry material. However, the brightness contrast would be expected to be strongest at shallow phase angles and absent at phase angles around 130 deg. Additionally, contrast might be stronger at short visible wavelengths than at NIR wavelengths. Although a detection of these signatures would not prove the presence of liquid water, they might be useful for constraining interpretations of surface contrast that, if found, are suggestive of liquid water's presence.

References: [1] Mellon M. T. and Jakosky B. M. (1995) *JGR*, 100, 11781–11799. [2] Feldman W. C. et al. (2002) *Science*, 297, 75–78. [3] Mitrofanov et al. (2002) *Science*, 297, 78–81. [4] Boynton et al. (2002) *Science*, 297, 81–85. [5] Haberle R. M. et al. (2001) *JGR*, 106, 23317–23326. [6] Sears D. W. G. and Chittenden J. D. (2005) *GRL*, 32, 23203. [7] Garvin J. B. et al. (2000) *Icarus*, 145, 648–652. [8] Márquez A. et al. (2004) *Icarus*, 172, 573–581. [9] Allen C. C. et al.

(1997) *LPS XXVIII*, Abstract#1797. [10] Gunderson K. et al. (2006) *Planet. Space Sci.*, in press. [11] McEwen A. S. et al. (2006) *JGR*, in press. [12] Hapke B. (1993) *Theory of reflectance and emittance spectroscopy*. University Press: Cambridge. [13] Mustard J. F. and Bell J. F. (1994) *GRL*, 21, 353–356.

Acknowledgements: This work has been funded through a grant from the Swiss National Fond.

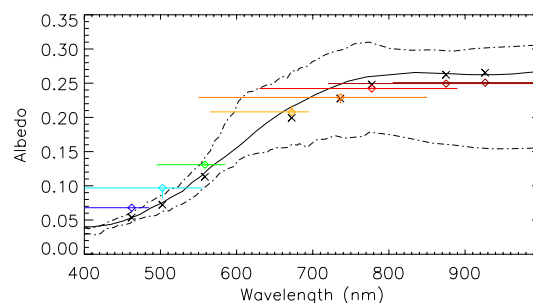


Figure 4. Dry simulant albedo measurements (diamonds) with filter FWHM bandpasses overplotted as horizontal bars and systematic errors as vertical bars. Colors are the same as Figures 1 and 2. Solid: simulant spectrum according to [9]. X's: Spectrum of [9] run through the PHIRE instrument response model. Dot-dash: Typical spectra of bright and dark Martian terrains [13].

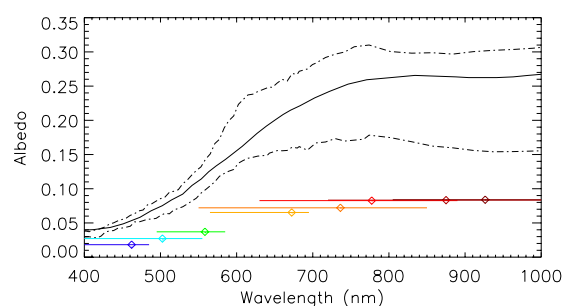


Figure 5. Same as Figure 4, but for the wet simulant.

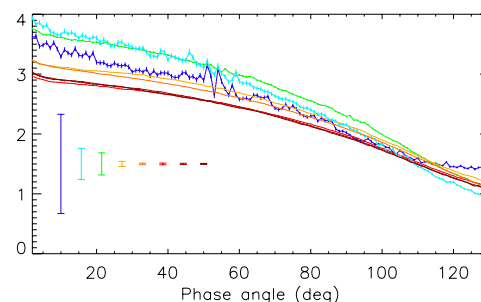


Figure 6. Dry:wet BRDF ratios. Statistical errors are overplotted as horizontal lines, and systematic errors are shown as error bars in the lower left.